JOURNAL OF MAGNETIC RESONANCE **127,** 80–86 (1997)
ARTICLE NO. MN971182

Use of RF Gradients in Excitation Sculpting, with Application to 2D HSQC

Sami Heikkinen,* Erkki Rahkamaa,* and Ilkka Kilpeläinen†

*Department of Chemistry, University of Oulu, FIN-90570 Oulu, Finland;
and †Institute of Biotechnology, University of Helsinki, P.O. Box 56, FIN-00014 Helsinki, Finland

Received November 12, 1996; revised April 16, 1997

The gradient pulses of double-GBIRD can be replaced with high-power spin-lock pulses (RF gradients) in *z*-rotation composite sandwiches. Implementation of this double-spin-locked BIRD (double-SLBIRD) in 2D HSQC results in drastic suppression of t_1 noise, nice baseline characteristics, and good dynamic range. The superior properties of double-SLBIRD-HSQC over conventional HSQC and even over double-spin-locked HSQC for small to medium-sized molecules makes this excitation-sculpting approach preferable. However, double-SLBIRD should not be considered as an alternative for double-GBIRD, but rather as a substitute for those spectrometers lacking field gradients.

INTRODUCTION

Selection of ^{13}C-bound protons with high suppression ratio of parent-proton signals (excitation sculpting) can be achieved by applying proton spin-lock pulses that have been implemented in *z*-rotation composite sandwiches on both sides of BIRD pulses. This paper describes the principles of this double-spin-locked BIRD (double-SLBIRD) sequence and its application to 2D HSQC. The double-SLBIRD is basically similar to double-GBIRD (*1–3*), but the gradient pulses have been replaced with high-power proton spin-lock pulses (RF gradients) (*4, 5*). It should be noted that the double-SLBIRD is not an alternative to double-GBIRD, but rather a substitute for those spectrometers not having field gradients. Implementation of double-SLBIRD in the 2D HSQC sequence (replacing the first 90° excitation pulse) results in drastic suppression of t_1-noise ridge intensities, nice baseline characteristics, and the possibility to use large receiver gain.

Double pulsed-field-gradient spin echo with BIRD pulses (*6*) as a refocusing pulse for ^{13}C-bound protons is an efficient method for suppressing strong parent-proton signals (double-GBIRD) (*1–3*). As both ^{13}C-bound protons and carbons are flipped, the $J(^{13}\mathrm{C}, ^{1}\mathrm{H})$ continues evolution after the first GBIRD cluster. To eliminate this, an inversion pulse for carbons is applied between the two GBIRD clusters. The suppression ratio of this double-GBIRD is about 50–200 (*2, 3*). This means that after double-GBIRD the parent signals are only 2–4 times stronger than the satellites. Complete suppression, as in case of quad-GBIRD [suppression ratio about 100 times better than with double-GBIRD (*2, 3*)], is usually not necessary for proton-detected two-dimensional techniques, as the final suppression of parent signals can be achieved successfully with phase cycling.

The double-GBIRD-type experiment can be performed by using high-power proton spin-lock pulses on both sides of the BIRD clusters (double-SLBIRD, Fig. 1). In our application, the spin-lock pulses embracing the BIRD clusters wereimplemented in *z*-rotation sandwiches (90°_{ψ}—$\mathrm{SL}_{\psi+\pi/2}$—$90^\circ_{-\psi}$) (*5, 7*). This causes the magnetization to be dispersed in the *xy* plane due to B_1-field inhomogeneity; i.e., the B_1 gradients have the same effect as conventional B_0 gradients do.

THEORY

The product operator calculations (*8*) for double-SLBIRD sequence (Fig. 1) were carried out for an isolated $^{1}\mathrm{H}^{13}\mathrm{C}$ pair and for a $^{1}\mathrm{H}^{1}\mathrm{H}$ pair. The integrations were carried out rejecting TOCSY and ROESY transfer, and were verified with POMA (*9*). The TOCSY and ROESY transfer may cause spurious correlations in some applications, but if the mixing times are kept short, these effects are small. Most of the calculation steps for the isolated $^{1}\mathrm{H}^{13}\mathrm{C}$ pair during the first SLBIRD cluster are shown for the sake of clarity. The integral is taken from 0 to 2π for the SL1 pulse.

The operator shown in Eq. [1] represents the surviving magnetization of an isolated $^{1}\mathrm{H}^{13}\mathrm{C}$ pair. The intensity of the signals is dependent on the multiplier of operator H_y and for

1090-7807/97 $25.00

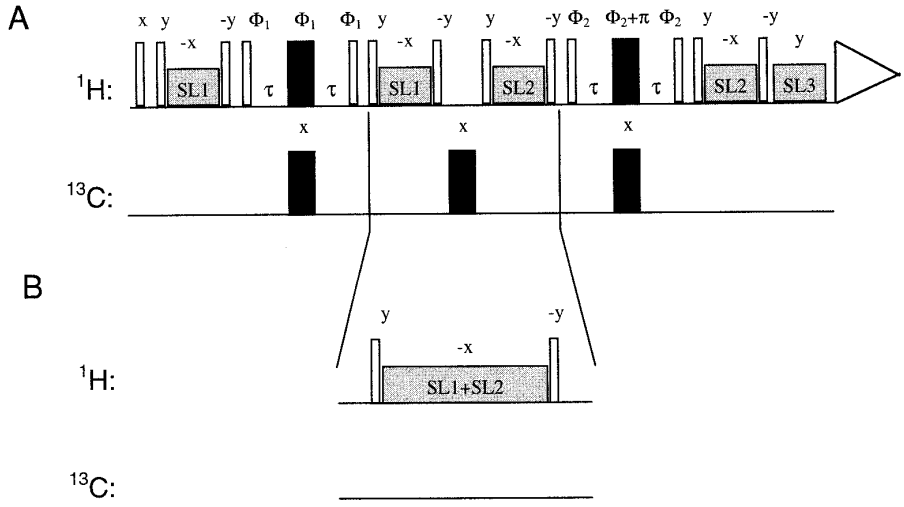

FIG. 1. Pulse sequence for the double-SLBIRD experiment. Sequence (A) is similar to double-GBIRD. Only B_0 gradients are replaced. In sequence (B), the carbon 180° has been omitted and the spin-lock pulses in the middle have been combined. Narrow bars and filled black bars indicate 90° and 180° hard rectangular pulses. Spin-lock pulses are presented with wide gray bars denoted by SL. Basic phase cycle: $\Phi_1 = x, y, -x, -y$; $\Phi_2 = 4(x), 4(y), 4(-x), 4(-y)$; receiver $= 2(x, -x, x, -x, -x, x, -x, x)$. Delay τ is tuned to $1/2J(^1\text{H}, ^{13}\text{C})$. Other interpulse delays are kept as short as possible.

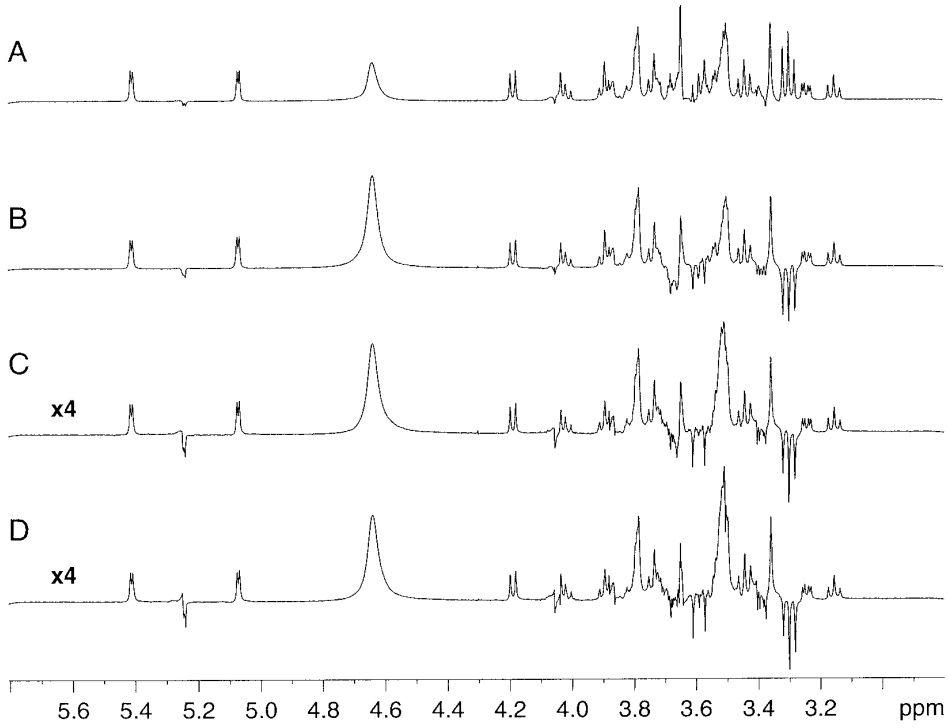

FIG. 2. The double-GBIRD with purge spin lock prior to acquisition (A) and three double-SLBIRD spectra (B–D) of 0.5 *M* sucrose in D_2O at 298 K. Experimental parameters: $\tau = 2.94$ ms. (A) Acquisition time = 1.36 s, gradient pulse length = 1 ms, gradient recovery time = 500 μs, gradient shape = sinusoid, amplitudes for two sets of gradients = 7.2 and 3 G/cm, length of purge spin-lock pulse = 1 ms, number of scans = 16. (B–D) Acquisition time = 1.36 s, SL1 = 1.4 ms, SL2 = 1.8 ms, length of purge spin-lock pulse = 1.0 ms, number of scans = 16 (B), 4 (C, D). Spectra (B, C) were recorded using the sequence in Fig. 1A, and spectrum (D) was recorded using the sequence in Fig. 1B. The FIDs were zero filled and multiplied by an exponential function (line broadening of 0.3 Hz) prior to Fourier transformation.

an optimum case [i.e., τ set equal to $1/2J(^{13}C, ^{1}H)$] the intensity is -1:

$$H_z \xrightarrow{H(90°)_x} -H_y$$

$$\xrightarrow{H(90°)_y\text{—}(SL1)_{-x} - H(90°)_{-y}}$$

$$-H_y\cos SL1 - H_x\sin SL1$$

$$\xrightarrow{BIRD} -H_y\cos SL1$$

$$-H_x\sin SL1\cos 2\pi J_{CH}\tau + 2H_zC_y\sin SL1\sin 2\pi J_{CH}\tau$$

$$\xrightarrow{H(90°)_y - (SL1)_{-x} - H(90°)_{-y}} -H_y\cos^2 SL1$$

$$-H_x\cos SL1\sin SL1 - H_x\cos SL1\sin SL1$$

$$\times\cos 2\pi J_{CH}\tau + H_y\sin^2 SL1\cos 2\pi J_{CH}\tau$$

$$+ 2H_zC_y\sin SL1\sin 2\pi J_{CH}\tau$$

$$\xrightarrow{\text{Integration}} -0.5H_y + 0.5\cos 2\pi J_{CH}\tau H_y$$

$$\xrightarrow{SLBIRD}$$

$$\xrightarrow{\text{Integration}} [-0.25 + 0.5\cos 2\pi J_{CH}\tau$$

$$-0.25\cos^2 2\pi J_{CH}\tau]H_y \Leftrightarrow \quad [1]$$

$$-(-0.5 + 0.5\cos 2\pi J_{CH}\tau)^2 H_y.$$

The operator in Eq. [2] represents the resulting magnetization of a ^{12}C-bound proton with one homonuclear coupling $J(^{1}H_1, ^{1}H_2)$. The terms representing observable magnetization of the proton to which the proton of interest is coupled (resulting from COSY-type transfer) are not shown.

$$H_z \xrightarrow{\text{double-SLBIRD}} [-0.25 + 0.5\cos 2\pi J_{HH}\tau$$

$$-0.25\cos 4\pi J_{HH}\tau]H_y + [-0.25\sin 2\pi J_{HH}\tau$$

$$+ 0.125\sin 4\pi J_{HH}\tau]H_{1x}H_{2z}. \quad [2]$$

Equation [2] shows that even one homonuclear coupling spoils the complete suppression of parent signals. The situation is similar to that with double-GBIRD, as trigonometric terms with even power describing z pulses of duration t_g (B_0 gradients of length t_g) are nonvanishing.

EXPERIMENTAL

All spectra were recorded on a Bruker DRX-500 NMR spectrometer (500 MHz ^{1}H frequency) equipped with a Bruker triple-resonance probe and z-axis gradient system, at 298 K. The length of a 90° pulse on high power level was 5.5 μs. Thus, during the spin-lock pulses (durations: SL1 = 1.4 ms, SL2 = 1.8 ms, and SL3 = 1.0 ms), a proton on resonance undergo 45–64 rotations. The probe inhomogeneity was measured with successive rotations to give intensity ratios of 1.00:0.89:0.79:0.70 with 90°, 450°, 810°, and 1170° pulses, respectively. The 0.5 M sucrose sample was prepared by dissolving sucrose (not D exchanged) in 0.7 ml of 99.5% D_2O.

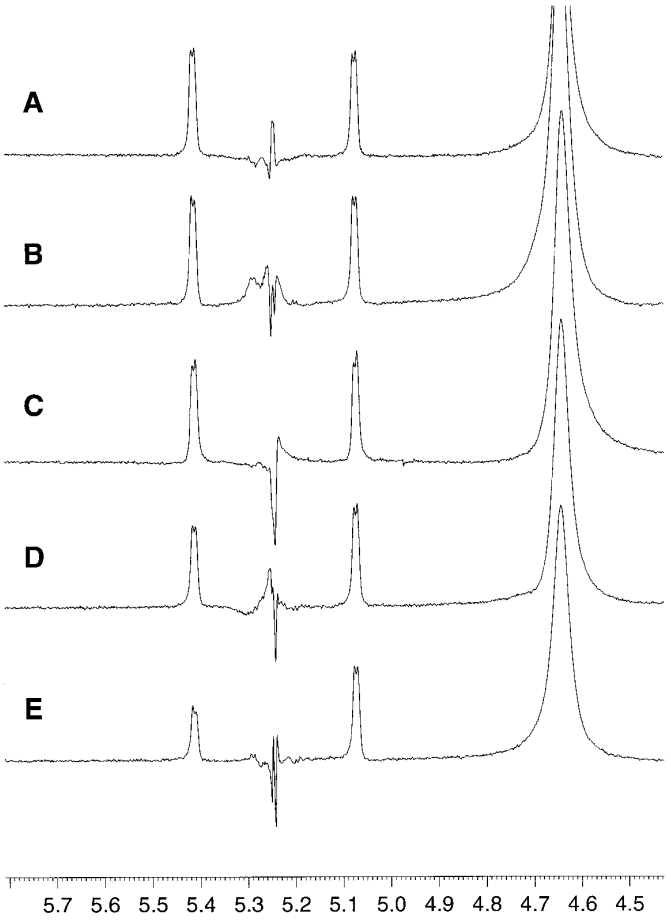

FIG. 3. Effect of transmitter offset on suppression performance of double-SLBIRD. The transmitter was placed at 11.0 (A), 8.00 (B), 5.00 (C), 2.00 (D), and −1.00 ppm (E) while observing the anomeric proton region. The transmitter offset effects do not significantly interfere with the suppression performance of double-SLBIRD.

RESULTS AND DISCUSSION

In principle, the carbon inversion pulse between the two SLBIRD clusters (Fig. 1A) can be omitted as no evolution takes place during the spin-lock gradients. The $^{1}H-^{13}C$ coupling evolution is active during the interpulse delays, but in practice this evolution is insignificant since the delays are

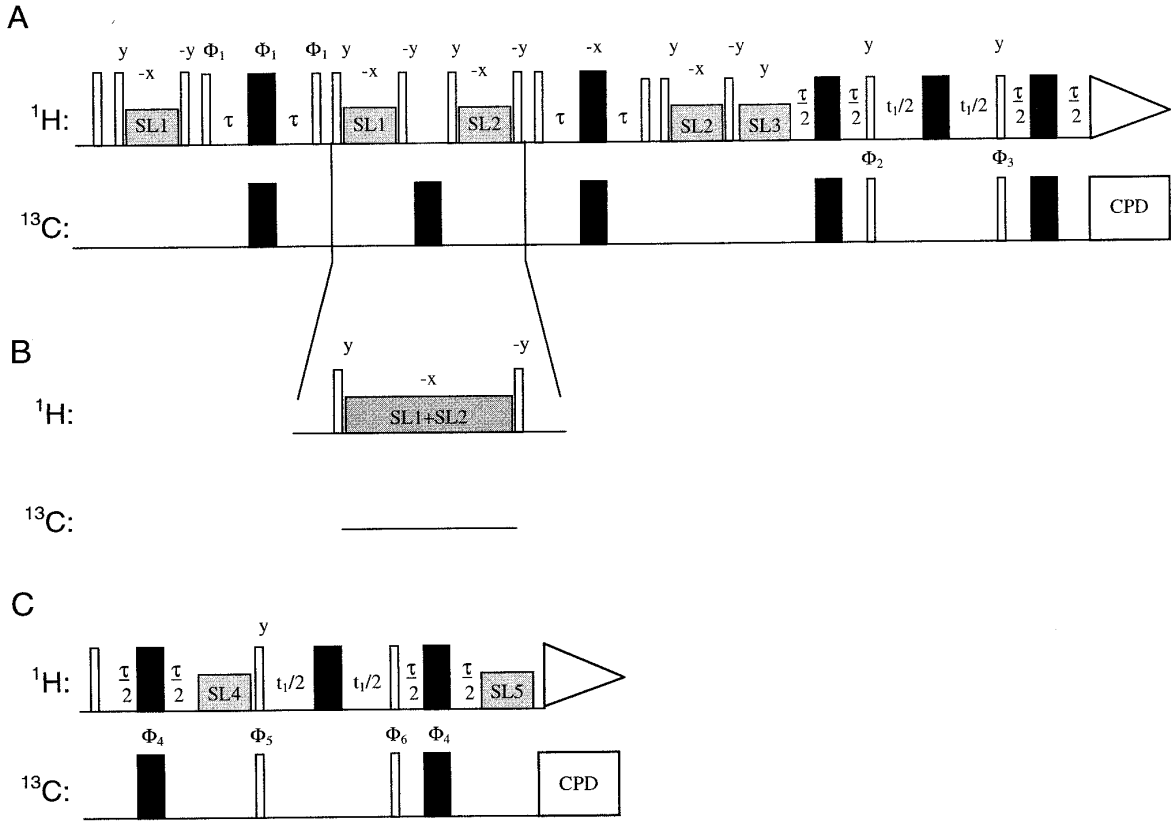

FIG. 4. Pulse sequences for double-SLBIRD-HSQC (A, B) and double-spin-locked HSQC (C) experiments. In sequence (B), the carbon inversion pulse is omitted and the two middle spin-lock pulses are combined. Narrow bars and filled black bars indicate 90° and 180° pulses. Spin-lock pulses are indicated by SL. Composite pulse decoupling on carbon during acquisition is indicated by CPD. Unless indicated differently, all the pulses are applied along the x axis. Basic phase cycle for BIRD-based sequences: $\Phi_1 = x, y, -x, -y$; $\Phi_2 = 4(x), 4(-x)$; $\Phi_3 = 8(x), 8(-x)$; receiver $= (x, -x, x, -x), 2(-x, x, -x, x), (x, -x, x, -x)$. Phase cycle used for spin-locked and conventional HSQC: $\Phi_4 = 4(x), 4(-x)$; $\Phi_5 = x, -x$; $\Phi_6 = 2(x), 2(-x)$; receiver $= x, -x, -x, x$. The phase of 90° carbon pulse prior to the t_1 period is subject to TPPI incrementation (*13*). The fixed delay τ is tuned to $1/2^1J(^1\mathrm{H}, ^{13}\mathrm{C})$. Other interpulse delays are kept as short as possible.

short. Therefore, it is possible to combine the two spin-lock pulses between the BIRD pulses and omit the carbon inversion pulse, as shown in Fig. 1B. As for gradients in double-GBIRD, the spin locks SL1, SL2, and SL3 should be of different length to avoid possible refocusing of the unwanted magnetization. The spin lock SL3 is used just for purging all the magnetization that is not along y axis before the acquisition.

Comparison between double-GBIRD and the two double-SLBIRDs is shown in Fig. 2. Both BIRD pulses were phase cycled independently using EXORCYCLE (*10*) to reinforce the echo. The spectrum in Fig. 2C is a result of double-SLBIRD with only the first BIRD being phase cycled. The spectrum in Fig. 2D was recorded using the sequence in Fig. 1B applying the EXORCYCLE on the first BIRD pulse. The properties of the spectrum recorded with the sequence in Fig. 1A (Fig. 2C vs 2B) do not change significantly, making a four-step phase cycle usable. Omitting the carbon inversion pulse (Fig. 1A vs 1B) does not interfere with spectral quality (Fig. 2C vs 2D). All the experiments in Fig. 2 were performed using identical parameters, except for the number of scans for spectra in Figs. 2C and 2D (see legend of Fig. 2).

The effect of homonuclear $J(^1\mathrm{H}, ^1\mathrm{H})$ on suppression of the parent-proton signals is clearly visible in Figs. 2A–2D. The suppression is fine for the anomeric proton signal as there is only one $J(^1\mathrm{H}, ^1\mathrm{H}) = 3.85$ Hz evolving during the BIRD pulses. However, the residual parent signal of a more strongly coupled proton at 3.3 ppm [triplet, two $J(^1\mathrm{H}, ^1\mathrm{H}) = 9.45$ Hz couplings] is of significant magnitude. In the double-SLBIRD spectra (Figs. 2B–2D), the residual parent signals appear as negative signals, whereas in the double-GBIRD spectra (2A) they are positive. It is noteworthy that the residual signals are of similar magnitude in both cases.

In principle, the strength of the RF gradients are quite strongly dependent on transmitter offset. We tested this phenomenon by moving the transmitter offset to different loca-

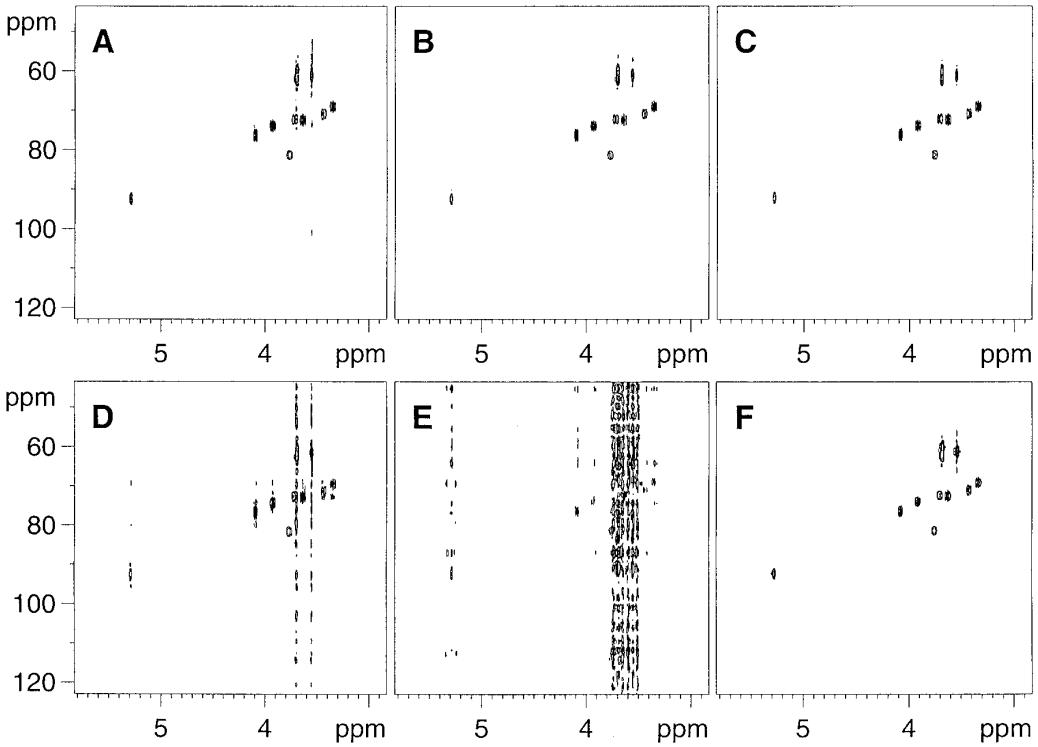

FIG. 5. Contour plots of phase-sensitive 2D spectra of 0.5 sucrose in D_2O. The experimental parameters are given in the legend to Fig. 4. (A) Double-SLBIRD-HSQC (pulse sequence in Fig. 4A), (B) double-SLBIRD-HSQC (pulse sequence in Fig. 4B), (C) double-GBIRD-HSQC (*1*), (D) double-spin-locked HSQC (*11*), (E) conventional HSQC, and (F) gradient-selected HSQC (*12*). All spectra are plotted with the same relative scale. Note the low intensity of t_1-noise ridges in spectra (A–C).

tions (−1.00 to −11.00 ppm), while observing the residual parent signal of the anomeric proton (Fig. 3). It can be concluded from Fig. 3 that the double-SLBIRD suppression is working properly with normal spectral widths.

The implementation of double-SLBIRD in a 2D HSQC sequence (replacing the first 90° pulse) is straightforward. The basic pulse sequence for double-SLBIRD-HSQC is shown in Fig. 4A. In addition, a modification of the double-SLBIRD-HSQC was made by omitting the carbon pulse between the two SLBIRD clusters and combining the spin-lock pulses, as shown in Fig. 4B. In double-SLBIRD-HSQC, EXORCYCLE (*10*) was applied to the first BIRD element (*1*). This means that 16 transients were to be taken for one time increment to complete both the EXORCYCLE and the basic four-step phase cycling of the HSQC.

Comparisons were made among double-SLBIRD-HSQC, double-GBIRD-HSQC [basically similar to HMQC in Ref. (*2*)], double-spin-locked-HSQC (*11*), conventional HSQC, and gradient-selected HSQC (*12*). The pulse sequence used for double-spin-locked-HSQC is shown in Fig. 4C.

Figure 5 presents a series of 2D HSQC spectra of 0.5 *M* sucrose in D_2O. The spectra were recorded with double-SLBIRD-HSQC (Figs. 5A and 5B), double-GBIRD-HSQC (*2*) (Fig. 5C), double-spin-locked-HSQC (Fig. 5D), conventional HSQC (Fig. 5E), and gradient-selected HSQC (Fig. 5F) pulse sequences. All 2D spectra are plotted using the same relative scale. The magnitude of t_1 noise is clearly smallest in Figs. 5B and 5C.

In Fig. 6, slices taken from the above-mentioned 2D HSQC spectra (along F_1) at anomeric carbon resonance are shown. The slices from the double-SLBIRD-HSQC have signal-to-t_1-noise ratios of 51.7 (Fig. 6A) and 70.8 (Fig. 6B). It is noteworthy that the removal of the carbon inversion pulse (see Fig. 4A vs 4B) increases the signal-to-t_1-noise ratio considerably. The S/N ratio of the double-SLBIRD-HSQC (Fig. 5B) is slightly smaller than that of the double-GBIRD-HSQC (Fig. 6C, ratio = 81.3), comparable to gradient-selected HSQC (Fig. 6F, ratio = 69.4), and much better than that of conventional HSQC (Fig. 6E, ratio = 4.0) and that of double-spin-locked HSQC (Fig. 6D, ratio = 14.2). The S/N ratio of double-SLBIRD recorded with 2 scans was 16.5, slightly better than that of double-spin-locked HSQC recorded with 16 scans. The signal-to-t_1-noise ratio was calculated using signal region 5.4–5.1 ppm and t_1-noise region 4.5–3.0 ppm. In addition, the baseline is flat in Figs. 6A and 6B (and Fig. 6C), whereas in Fig. 6F large distortions can be found at the base of the anomeric proton resonance. This distortion is a result of simultaneous disa-

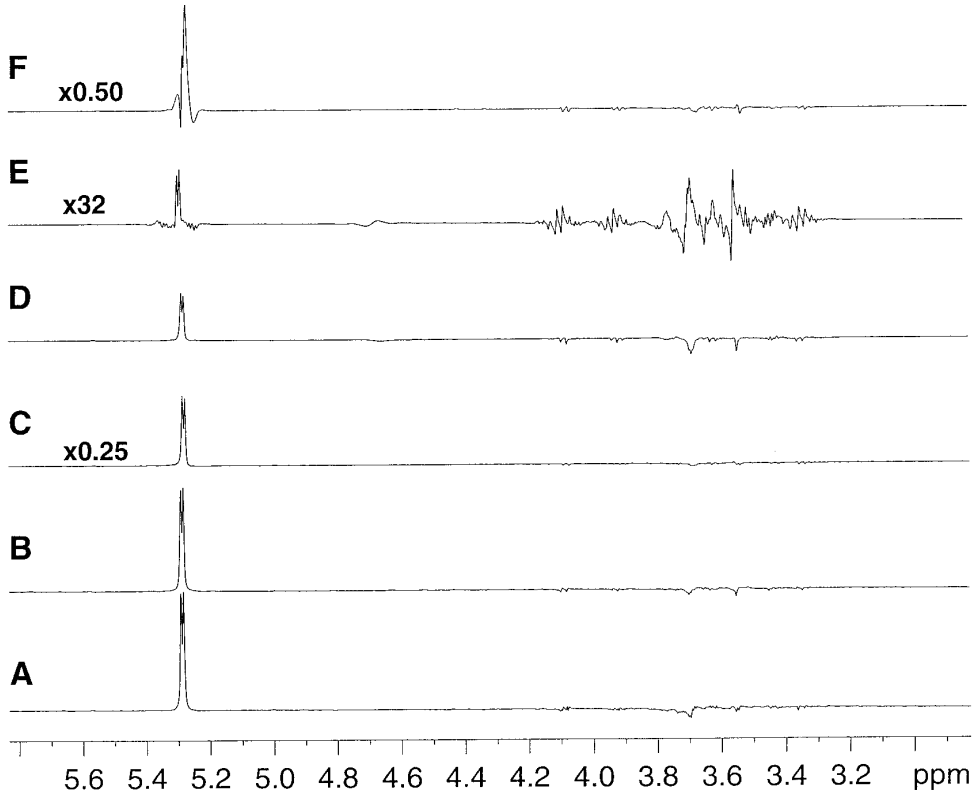

FIG. 6. The anomeric carbon slices of 2D spectra in Fig. 5 recorded using phase-sensitive sequences: (A) double-SLBIRD-HSQC (pulse sequence in Fig. 3A), (B) double-SLBIRD-HSQC (pulse sequence in Fig. 3B), (C) double-GBIRD-HSQC (*1*), (D) double-spin-locked HSQC (*11*), (E) conventional HSQC, and (F) gradient-selected HSQC (*12*). Sample: 0.5 *M* sucrose in D_2O at 298 K. Experimental parameters: Bruker DRX-500 NMR spectrometer equipped with Bruker triple-resonance probe and *z*-axis gradient system, 500 MHz ^{1}H frequency, τ = 3.45 ms, relaxation delay = 1.5 s, t_{1max} = 3.2 ms, t_2 = 681.6 ms, carbon decoupling by GARP (*14*), number of transients = 16, number of time increments = 64, gradient pulse length = 1 ms, gradient recovery time = 200 μs, gradient shape = sinusoid; (A, B) SL1 = 1.4 ms, SL2 = 1.8 ms, SL3 = 1.0 ms; (C) gradient amplitudes = 7.2, 7.2, 3.0, and 3.0 G/cm; (D) SL4 = 1.4 ms, SL5 = 1.8 ms; (F) gradient amplitudes = 24.0, 9.0, and 6.0 G/cm. The t_1 domain was zero filled twice and the t_2 domain was zero filled once, and both dimensions were multiplied with a cosine function prior to Fourier transformation.

bling of the gradient and enabling of the lock just prior to acquisition. This could be circumvented by enabling the lock after the acquisition or by careful timing of gradient disabling and lock enabling. Dynamic-range properties are also good for the double-SLBIRD-HSQC sequence, which allowed us to use receiver gains about 44 and 8 dB larger than those used in conventional HSQC and in double-spin-locked HSQC, respectively. In addition, the receiver gain in double-SLBIRD-HSQC was 9 dB smaller than that in gradient-selected HSQC and 7 dB smaller than that in double-GBIRD-HSQC.

CONCLUSIONS

Since the lock system can remain engaged throughout the double-SLBIRD experiment and the suppression of the parent signals with double-SLBIRD is approximately of same order as that for double-GBIRD, the SLBIRD approach can be found useful. In addition, the baseline properties are the same, and specially no hardware modifications are needed. Thus we find the double-SLBIRD method usable for spectrometers lacking a pulsed-field-gradient accessory.

The superior properties of double-SLBIRD-HSQC over the conventional HSQC and even over the double-spin-locked HSQC for small to medium-sized molecules makes this excitation sculpting approach preferable, if field gradients are not available. With larger molecules, the double-SLBIRD sequence prior to the HSQC sequence may result in significant decrease in signal intensity due to short T_2 relaxation times of protons.

REFERENCES

1. T. L. Hwang and A. J. Shaka, *J. Magn. Reson. A* **112,** 275 (1995).
2. C. Emetarom, T. L. Hwang, G. Mackin, and A. J. Shaka, *J. Magn. Reson. A* **115,** 137 (1995).

3. G. Mackin and A. J. Shaka, *J. Magn. Reson. A* **118,** 247 (1996).
4. C. J. R. Counsell, M. H. Levitt, and R. R. Ernst, *J. Magn. Reson.* **64,** 470 (1985).
5. W. E. Maas, F. Laukien, and D. G. Cory, *J. Magn. Reson. A* **103,** 115 (1993).
6. J. R. Garbow, D. P. Weitekamp, and A. Pines, *Chem. Phys. Lett.* **93,** 504 (1982).
7. R. Freeman, T. A. Frenkiel, and M. H. Levitt, *J. Magn. Reson.* **44,** 409 (1981).
8. (*a*) O. W. Sørensen, G. W. Eich, M. H. Levitt, G. Bodenhausen, and R. R. Ernst, *Prog. NMR Spectrosc.* **16,** 163 (1983); (*b*) S. Wolfram, ''Mathematica. A System for Doing Mathematics by Computer,'' Addison-Wesley, Redwood City, California, 1988.
9. P. Güntert, N. Schaefer, G. Otting, and K. Wüthrich, *J. Magn. Reson. A* **101,** 470 (1985).
10. G. Bodenhausen, R. Freeman, and D. L. Turner, *J. Magn. Reson.* **27,** 511 (1977).
11. G. Otting and K. Wüthrich, *J. Magn. Reson.* **76,** 569 (1988); W. E. Maas and D. G. Cory, *J. Magn. Reson. A* **112,** 229 (1995).
12. W. Willker, D. Leibfritz, R. Kerssebaum, and W. Bermel, *Magn. Reson. Chem.* **31,** 287 (1993).
13. D. Marion and K. Wütrich, *Biochem. Biophys. Res. Commun.* **113,** 967 (1983).
14. A. J. Shaka, P. B. Barker, and R. Freeman, *J. Magn. Reson.* **64,** 547 (1985).